Article

High Anisotropy of the Field-Effect Transistor Mobility in Magnetically Aligned Discotic Liquid-Crystalline Semiconductors

Igor O. Shklyarevskiy, Pascal Jonkheijm, Natalie Stutzmann, Dorothee Wasserberg, Harry J. Wondergem, Peter C. M. Christianen, Albertus P. H. J. Schenning, Dago M. de Leeuw, eljko Tomovi, Jishan Wu, Klaus Mllen, and Jan C. Maan

J. Am. Chem. Soc., **2005**, 127 (46), 16233-16237• DOI: 10.1021/ja054694t • Publication Date (Web): 22 October 2005

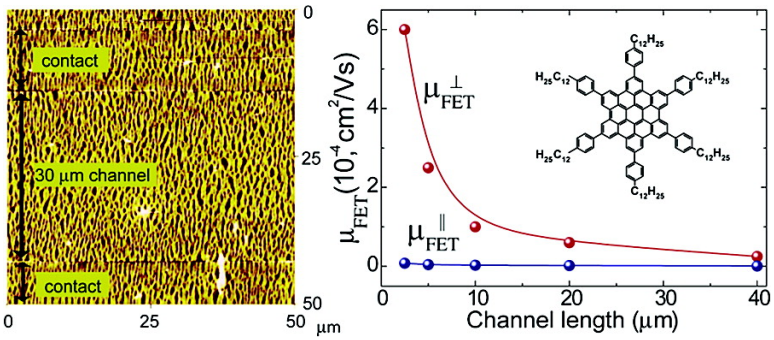

More About This Article

Additional resources and features associated with this article are available within the HTML version:

- Supporting Information
- Links to the 18 articles that cite this article, as of the time of this article download
- Access to high resolution figures
- Links to articles and content related to this article
- Copyright permission to reproduce figures and/or text from this article

View the Full Text HTML

J|A|C|S
ARTICLES
Published on Web 10/22/2005

High Anisotropy of the Field-Effect Transistor Mobility in Magnetically Aligned Discotic Liquid-Crystalline Semiconductors

Igor O. Shklyarevskiy,[†,‡] Pascal Jonkheijm,[‡] Natalie Stutzmann,[§] Dorothee Wasserberg,[‡] Harry J. Wondergem,[§] Peter C. M. Christianen,*[,†] Albertus P. H. J. Schenning,*[,‡] Dago M. de Leeuw,[§] Željko Tomović,[⊥] Jishan Wu,[⊥] Klaus Müllen,*[,⊥] and Jan C. Maan[†]

Contribution from the High Field Magnet Laboratory, Institute for Molecules and Materials, Radboud University Nijmegen, Toernooiveld 7, 6525 ED Nijmegen, The Netherlands, Laboratory of Macromolecular and Organic Chemistry, Eindhoven University of Technology, P.O. Box 513, 5600 MB Eindhoven, The Netherlands, Philips Research Laboratories, Prof. Holstlaan 4, 5656 AA, Eindhoven, The Netherlands, and Max Planck Institute for Polymer Research, Ackermannweg 10, 55128, Mainz, Germany

Received July 14, 2005; E-mail: p.christianen@science.ru.nl; a.p.h.j.schenning@tue.nl; muellen@mpip-mainz.mpg.de

Abstract: A magnetic field has been utilized for producing highly oriented films of a substituted hexabenzocoronene (HBC). Optical microscopy studies revealed large area HBC monodomains that covered the entire film, while wide-angle X-ray measurements showed that the HBC molecules are aligned with their planes along the applied field. On the basis of this method, solution-processed field-effect transistors (FET) have been constructed with charge carrier mobilities of up to 10^{-3} $cm^2/V\cdot s$, which are significantly enhanced with respect to the unaligned material. Exceptionally high mobility anisotropies of 25−75 for current flow parallel and perpendicular to the alignment direction have been measured as a function of the channel length. Atomic force microscopy performed on the FET structures reveals fibril superstructures that are oriented perpendicularly to the magnetic field direction, consisting of molecular columns with a slippage angle of 40° between the molecules. For channel lengths larger than 2.5 μm, the fibrils are smaller than the electrode spacing, which adversely affects the device performance.

Introduction

Liquid-crystalline π-conjugated organic molecules are promising semiconductors for solution-based fabrication of electronic devices, such as field-effect transistors (FETs) and light-emitting diodes, due to the attractive prospect of harnessing their favorable capability for molecular self-assembly in mesophase(s). Mesoscopic order is of major importance for the electronic performance of organic semiconductors,[1] and alignment of the mesoscopic order may lead to enhanced charge-carrier mobility or to anisotropic optical or electrical properties.[2−5] Alignment techniques investigated so far include mechanical stretching,[6] Langmuir−Blodgett deposition,[7,8] and the use of alignment layers[3] or electric fields.[9] Here we demonstrate that high mesoscopic order can be introduced in thin films of a hexabenzocoronene-based discotic liquid crystal by application of a high magnetic field. This resulted in large-area monodomain films that allowed charge transport studies in FET devices, in which we found a more than 10-fold enhancement and an ultrahigh anisotropy, up to 75 times, of the field-effect mobility over unaligned films.

Magnetic alignment of an anisotropic molecule originates from the anisotropy in its diamagnetic susceptibility, χ, characterized by $\Delta\chi = \chi_{||} - \chi_{\perp}$, the difference in χ between two orthogonal molecular axes. The energy of a molecule, given by $E = -\chi B^2$,[10] therefore, depends on its orientation with respect to the magnetic field direction. An aromatic molecule, for instance, has a relatively high $\Delta\chi$ and tends to align with its ring plane, that is, the axis of lowest χ, along the magnetic field. It is not possible to align a single molecule with the highest

[†] Radboud University Nijmegen.
[‡] Eindhoven University of Technology.
[§] Philips Research Laboratories.
[⊥] Max Planck Institute for Polymer Research.

(1) Sirringhaus, H.; Brown, P. J.; Friend, R. H.; Nielsen, M. M.; Bechgaard, K.; Langeveld-Voss, B. M. W.; Spiering, A. J. H.; Janssen, R. A. J.; Meijer, E. W.; Herwig, P.; de Leeuw, D. M. *Nature* **1999**, *401*, 685−688.
(2) Sirringhaus, H.; Wilson, R. J.; Friend, R. H.; Inbasekaran, M.; Wu, W.; Woo, E. P.; Grell, M.; Bradley, D. D. C. *Appl. Phys. Lett.* **2000**, *77*, 406−408.
(3) Swiggers, M. L.; Xia, G.; Slinker, J. D.; Gorodetsky, A. A.; Malliaras, G. G.; Headrick, R. L.; Weslowski, B. T.; Shashidhar, R. N.; Dulcey, C. S. *Appl. Phys. Lett.* **2001**, *79*, 1300−1302.
(4) Nagamatsu, S.; Tanigaki, N.; Yoshida, Y.; Takashima, W.; Yase, K.; Kaneto, K. *Synth. Met.* **2003**, *137*, 923−924.
(5) Chen, X. L.; Lovinger, A. J.; Bao, Z.; Sapjeta, J. *Chem. Mater.* **2001**, *13*, 1341−1348.
(6) Dyreklev, P.; Berggren, M.; Inganas, O.; Andersson, M. R.; Wennerstrom, O.; Hjertberg, T. *Adv. Mater.* **1995**, *7*, 43−45.
(7) Cimrova, V.; Remmers, M.; Neher, D.; Wegner, G. *Adv. Mater.* **1996**, *8*, 146.
(8) Xu, G.; Bao, Z.; Groves, J. T. *Langumir* **2000**, *16*, 1834−1841.
(9) Mas-Torrent, M.; den Boer, D.; Durkut, M.; Hadley, P.; Schenning, A. P. H. J. *Nanotechnology* **2004**, *15*, S265−S269.
(10) Maret G.; Dransfeld K. *Physica* **1977**, *86−88B*, 1077−1083.

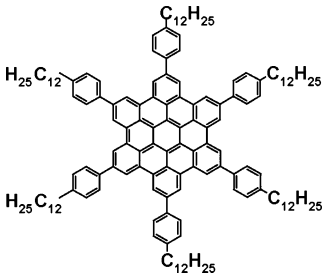

Figure 1. Chemical structure of the discotic liquid-crystalline semiconductor, hexa(4-dodecylphenyl)hexa-*peri*-hexabenzocoronene (HBC−PhC_{12}).

magnetic fields that are currently available since the reduction in magnetic energy, $\Delta\chi\ B^2$, is still considerably smaller than the thermal energy, kT (i.e., thermal motion prevents alignment). In a liquid-crystalline (LC) mesophase, however, the difference in magnetic energy of N self-assembled molecules can become large enough to align the molecules ($N\Delta\chi\ B^2 \gg kT$). Magnetic fields have been successfully utilized to align a wide variety of self-assembled systems.[11−16]

We selected hexa(4-dodecylphenyl)hexa-*peri*-hexabenzocoronene,[17] HBC−PhC_{12} (Figure 1), for the work reported here, as this material combines favorable magnetic and electrical properties. Their discotic LC phase and aromatic core, and thus high $\Delta\chi$ (4.9×10^{-9} m^3/mol),[18] make HBC derivatives suitable for magnetic alignment, while the formation of columnar stacks leads to one-dimensional charge-carrier transport.[19−21] High intrinsic charge-carrier mobilities have been found for HBC−PhC_{12} in time-resolved microwave conductivity measurements[21] and a mobility along the columnar stacks that is up to 20-times higher than perpendicular to them.[22] To date, this liquid-crystalline HBC derivative has never been applied in a FET. Different HBC derivatives, however, have been ordered, aligned, and used in FETs.[23−27] Charge-carrier mobilities, μ_{FE}, of up to

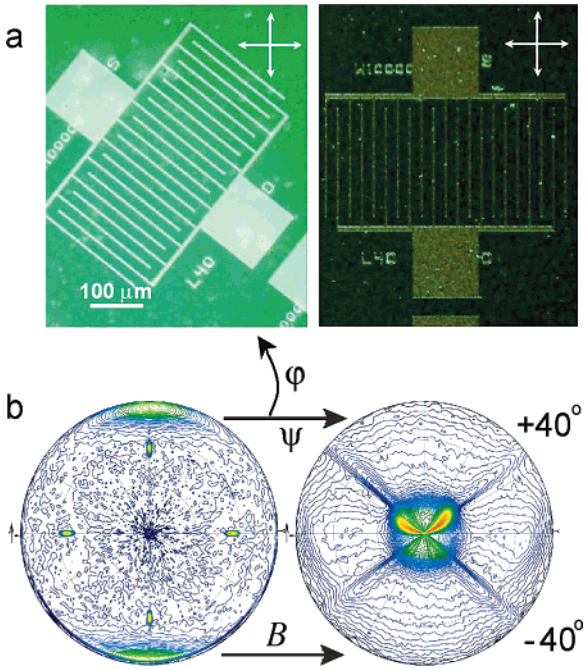

Figure 2. Structural characterization of magnetically aligned HBC−PhC_{12} films. (a) Optical micrographs under crossed polarizers. The transmitted light was maximal for films with the alignment direction at ±45° to the orientation of the polarizer/analyzer system (left), and minimal at 0 and 90° (right). (Arrows indicate the orientation of the polarizers.) (b) Wide-angle X-ray scattering pole figures measured as a function of φ (in-plane rotation around the center of the sample) and tilt angle ψ for two different scattering angles θ. Left*:* the pole figure measured at the *intra*columnar distance (0.35 nm, $2\theta = 25°$) reveals that the HBC−PhC_{12} molecules are oriented with their plane along the magnetic field. Right: probing at the *inter*columnar distance (3.4 nm, $2\theta = 2.5°$) reveals that the columnar stacks are at ±40° to the magnetic field axis.

1×10^{-2} $cm^2/V{\cdot}s$ were deduced for the zone-cast crystalline HBC,[25] while in devices based on films oriented on friction-transferred poly(tetrafluoroethylene),[26,27] mobility anisotropies for charge transport parallel and perpendicular to the HBC columns of 2 orders of magnitude were reported. We note, however, that this anisotropy might be due to the alignment layer that hampers perpendicular charge transport.[22,26]

Results and Discussion

Thin aligned films were prepared by casting a HBC−PhC_{12} solution (15 g/L in *p*-xylene) onto field-effect transistor test wafers positioned in a horizontal 20 T Bitter magnet at room temperature. During evaporation of the solvent, HBC−PhC_{12} undergoes a phase transition from the isotropic to a lyotropic LC phase. The actual alignment takes place when the columnar stacks are sufficiently large and mobile to be aligned.[14] The magnetic field was applied until the solvent had evaporated.

Remarkably, optical microscopy studies revealed large-area HBC monodomains that covered the *entire* FET substrate (Figure 2a). This is evidenced by the fact that transmitted light intensity maxima were observed for films positioned with the direction at which B was applied at ±45° to the polarizers, and minima for films with the B direction oriented parallel or perpendicular to them.

(11) de Gennes, P. G. *The Physics of Liquid Crystals* 79−95; Clarendon Press: Oxford, 1974.
(12) Ali-Adib, Z.; Davidson, K.; Nooshin, H.; Tredgold, R. H. *Thin Solid Films* **1991**, *201*, 187−195.
(13) Huser, B.; Spiess, H. W. *Makromol. Chem., Rapid Commun.* **1988**, *9*, 337−343.
(14) Boamfa, M. I.; Viertler, K.; Wewerka, A.; Stelzer, F.; Christianen, P. C. M.; Maan, J. C. *Phys. Rev. Lett.* **2003**, *90*, Art. No. 025501.
(15) Oguma, J.; Kawamoto, R.; Goto, H.; Itah, K.; Akagi, K. *Synth. Met.* **2001**, *119*, 537−538.
(16) Shklyarevskiy, I. O.; Christianen, P. C. M.; Schenning, A. P. H. J.; Meijer, E. W.; Henze, O.; Feast, W. J.; Maan J. C. *Mol. Cryst. Liq. Cryst.* **2004**, *410*, 551−556.
(17) (a) Fechtenkötter, A.; Saalwachter, K.; Harbison, M. A.; Mullen, K.; Spiess, H. W. *Angew. Chem., Int.* Ed. **1999**, *38*, 3039−3042. (b) Schmidt-Mende, L.; Fechtenkötter, A.; Müllen, K.; Moons, E.; Friend, R. H.; MacKenzie, J. D. *Science* **2001**, *293*, 1119−1122.
(18) Rogers, M. T. *J. Am. Chem. Soc.* **1947**, *69*, 1506−1508.
(19) Fischbach, I.; Pakula, T.; Minkin, P.; Fechtenkötter, A.; Müllen. K.; Spiess, H. W.; Saalwachter, K. *J. Phys. Chem. B* **2002**, *106*, 6408−6418.
(20) Lemaur, V.; da Silva Filho, D. A.; Coropceanu, V.; Lehmann, M.; Geerts, Y.; Piris, J.; Debije, M. G.; van de Craats, M.; Senthilkumar, K.; Siebbeles, L. D. A.; Warman, J. M.; Brédas, J.-L.; Cornil, J. *J. Am. Chem. Soc.* **2004**, *126*, 3271−3279.
(21) van de Craats, A. M.; Warman, J. M.; Fechtenkötter, A.; Brand, J. D.; Harbison, M. A.; Müllen. K. *Adv. Mater.* **1999**, *11*, 1469−1472.
(22) (a) Piris, J.; Debije, M. G.; Stutzmann, N.; van de Craats, A. M.; Watson, M. D.; Müllen, K.; Warman, J. M. *Adv. Mater.* **2003**, *15*, 1736−1740. (b) Piris, J.; Debije, M. G.; Stutzmann, N.; Laursen, B. W.; Pisula, W.; Watson, M. D.; Björnholm, T.; Müllen, K.; Warman, J. M. *Adv. Funct. Mater.* **2004**, *14*, 1053−1061.
(23) Reitzel, N.; Hassenkam, T.; Balashev, K.; Jensen, T. R.; Howes, P. B.; Kjaer, K.; Fechtenkötter, A.; Tchebotareva, N.; Ito, S.; Müllen, K.; Björnholm, T. H. *Chem.—Eur. J.* **2001**, *7*, 4894−4901.
(24) Tracz, A.; Jeszka, J. K.; Watson, M. D.; Pisula, W.; Müllen, K.; Pakula, T. *J. Am. Chem. Soc.* **2003**, *125*, 1682−1683.
(25) (a) Pisula, W.; Menon, A.; Stepputat, M.; Lieberwirth, I.; Kolb, U.; Tracz, A.; Sirringhaus, H.; Pakula, T.; Müllen, K. *Adv. Mater.* **2005**, *17*, 684−688. (b) Pisula, W.; Tomovic, Z.; Stepputat, M.; Kolb, U.; Pakula, T.; Müllen, K. *Chem. Mater.* **2005**, *17*, 2641−2647.
(26) van de Craats, A. M.; Stutzmann, N.; Bunk, O.; Nielsen, M. M.; Watson, M. D.; Müllen, K.; Chanzy, H. D.; Sirringhaus, H.; Friend, R. H. *Adv. Mater.* **2003**, *15*, 495−499.
(27) Bunk, O.; Nielsen, M. M.; Solling, T. I.; van de Craats A. M.; Stutzmann, N. *J. Am. Chem. Soc.* **2003**, *125*, 2252−2258.

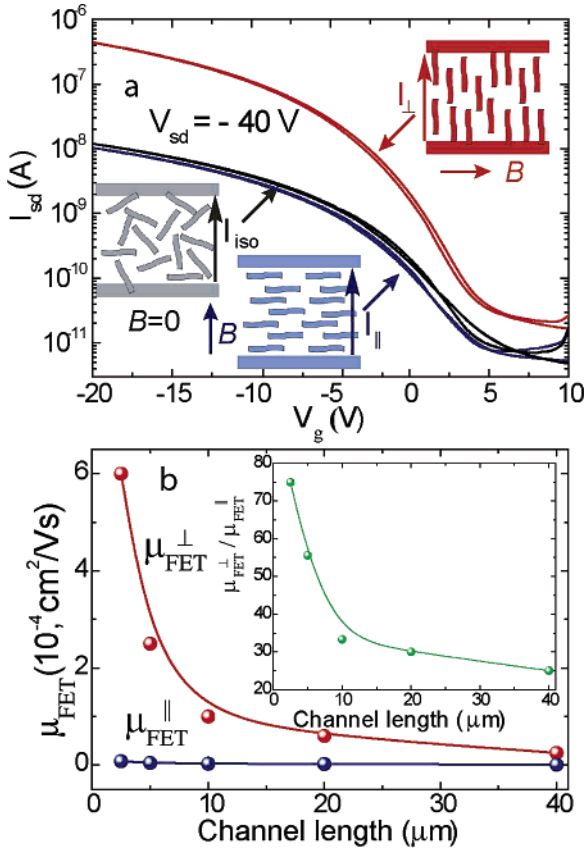

Figure 3. Electrical performance of a typical magnetically aligned HBC−PhC_{12}-based field-effect transistor (L = 10 μm and W = 10 mm). (a) Transfer characteristics for oriented HBC films, measured perpendicular ($I_\perp$, red line) and parallel ($I_{||}$, blue line) to the magnetic field direction, as well as active HBC layers prepared without application of a magnetic field (I_{iso}, black line). The insets schematically show the direction of the current with respect to the field direction B and HBC−PhC_{12} fibrils (see text and Figure 4). (b) Dependence of the field-effect mobility on the channel length for both current directions: $\mu_{FE}^{\perp}$ and $\mu_{FE}^{||}$ correspond to $I_\perp$ and $I_{||}$, respectively. Inset: channel length dependence of the anisotropy in the field-effect mobility ($\mu_{FE}^{\perp}/\mu_{FE}^{||}$).

To elucidate the molecular arrangement of HBC−PhC_{12} in more detail, wide-angle X-ray (WAXS) diffraction pole figure measurements were performed. Representative results are displayed in Figure 2b. The left pole figure was measured at the diffraction maximum originating from the intermolecular distance within a column (3.5 Å). It reveals that the HBC−PhC_{12} molecules are aligned with their planes along the applied magnetic field, as expected for an aromatic molecule, with the disc in an edge-on arrangement.[10] The two ridges in the right pole figure, corresponding to the WAXS intensity probed at the intercolumnar distance (3.44 nm), are likely due to the presence of domains with close-packed *molecular columns* making an angle of ±40° with the magnetic field direction (vide infra). Remarkably, magnetically aligned coronene cores have a ladder arrangement, which strongly contrasts all previous reports on HBC−PhC_{12} films[26,27] that show face-to-face stacking. The influence of the magnetic field on this difference in packing is the subject of further studies.

Unambiguous evidence for the high degree of molecular order introduced by the magnetic field was obtained from electrical characterization of devices with the charge transport direction parallel and perpendicular to the applied magnetic field (Figure 3a). These were compared with the performance of isotropic devices fabricated using the same procedure, but without a magnetic field applied. Typical transfer characteristics are shown in Figure 3a. All devices exhibited clean transistor action with high on−off current switching ratios up to 10^4 (measured between gate voltages $V_g = -20$ and 10 V), a good operating stability with typical turn-on voltages of ~5 V and negligible hysteresis between forward and backward scans. Most importantly, FETs with the charge transport direction perpendicular to the magnetic field displayed a substantially higher source−drain current than isotropic devices or devices with the channel parallel to the field. Extracting the respective saturated field-effect mobilities, μ_{FE},[28] with $\mu_{FE}^{\perp}$ and $\mu_{FE}^{||}$ = field-effect mobility perpendicular and parallel to the magnetic field, we find that $\mu_{FE}^{||} \approx \mu_{FE}^{iso} = 3 \times 10^{-6}$ cm^2/V·s and $\mu_{FE}^{\perp} = 10^{-4}$ cm^2/V·s (Figure 3b). Magnetic field alignment leads to a more than 10-fold enhancement of the mobility and a high anisotropy ($\mu_{FE}^{\perp}/\mu_{FE}^{||}$) of 33 ($L$ = 10 μm, W = 10 mm). This unequivocally demonstrates that the magnetic field alignment is effective in introducing one-dimensional mesoscopic order in the discotic liquid-crystalline semiconductors.

In addition, when analyzing the dependence of μ_{FE} with channel length, L, we find, rather surprisingly, that the anisotropy in the field-effect mobility ($\mu_{FE}^{\perp}/\mu_{FE}^{||}$) increases with decreasing L (W = const. = 10 mm), leading to a maximum anisotropy $\mu_{FE}^{\perp}/\mu_{FE}^{||} = 75$ for L = 2.5 μm (inset Figure 3b). This high anisotropy appears to be originating from the fact that higher values for $\mu_{FE}^{\perp}$ are recorded at smaller channel lengths, which is opposite to the more common behavior, where contact−resistance phenomena negatively affect μ_{FE} with decreasing L;[29] $\mu_{FE}^{\perp}$ increases more than 1 order of magnitude from 2.5×10^{-5} to 6×10^{-4} cm^2/V·s when reducing L from 40 to 2.5 μm. In this range, $\mu_{FE}^{||}$ was found to only change from 1×10^{-6} to 8×10^{-6} cm^2/V·s.

To gain more insight into this dependence, the microstructure of the magnetically aligned HBC films was investigated by tapping mode atomic force microscopy, performed directly on the FET structures. Representative images of FET devices with the channel perpendicular to the magnetic field direction (L = 30, 7.5, 5, and 3 μm, respectively) are displayed in Figure 4a−d, whereas Figure 4e displays a FET with a 3 μm long channel, with the channels oriented parallel to the magnetic field. Generally, we find that the aligned HBC−PhC_{12} films exhibit a *fibril* "superstructure" of individual "*fibrils*" oriented perpendicularly to the magnetic field direction. From the presented images, it appears that the highest field-effect mobility is obtained for devices of L = 2.5 μm as the gap between the electrodes is entirely covered by oriented HBC fibrils without dead ends. For larger L, the average length of the fibrils becomes smaller than the electrode spacing, which, eventually, will adversely affect device performance. Similarly, for devices with the magnetic field parallel to the channel, no continuous pathway is formed (Figure 4e). Nevertheless, the low values measured for $\mu_{FE}^{||}$, which are comparable to that of isotropic films (Figure 3b), may give some indication of the amount of molecular and microscopic defects and disorder present in the latter films.

Certainly, for all L values investigated, the average amount of fibril ends is much higher when the fibrils are aligned

(28) Sirringhaus, H.; Tessler, N.; Thomas, D. S.; Brown, P. J.; Friend, R. H. In *Advances in Solid State Physics 39*; Kramer, B., Ed.; Vieweg: Braunschweig 1999; pp 101−110.

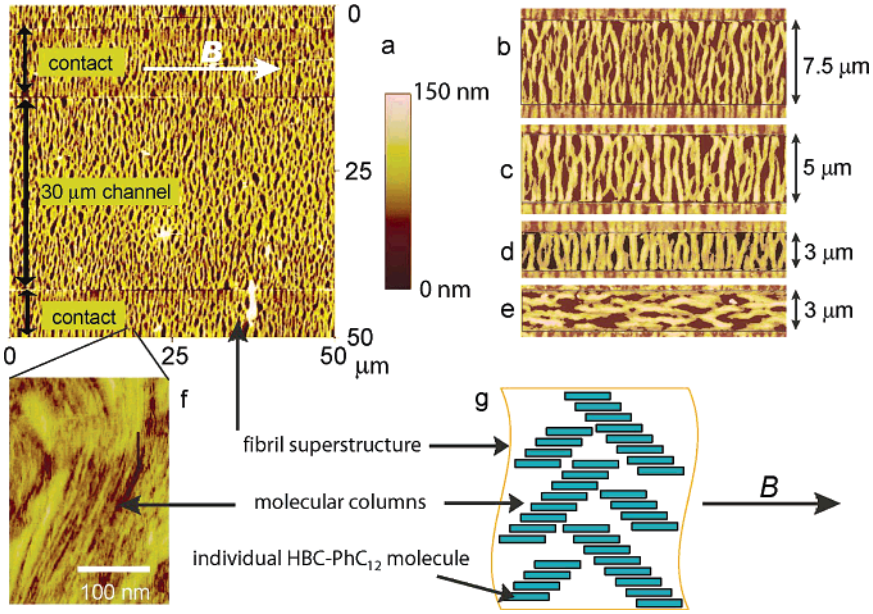

Figure 4. Atomic force microscopy (AFM) images of magnetically aligned HBC−PhC_{12}-based field-effect transistors for different channel lengths L and schematic representation of the fibril superstructure consisting of molecular columns: (a) $L = 30$ μm, (b) $L = 7.5$ μm, (c) $L = 5$ μm, (d) $L = 3$ μm, (e) $L = 3$ μm for the opposite orientation. (f) Internal structure of a fibril, showing evidence for unidirectionally aligned columnar stacks at 40° to the magnetic field. (g) Schematic representation (top view) of the fibril superstructure, aligned perpendicularly to the magnetic field. The fibrils consist of molecular columns at ±40° to the field, with the individual HBC−PhC_{12} molecules aligned along the field with the discs in an edge-on arrangement, which is consistent with the WAXS data (Figure 2b). The films in a−d are fabricated in a horizontal magnetic field (denoted by the black arrow). In e, the magnetic field direction is pointing upwards.

perpendicularly to the current path than for the parallel alignment (Figure 4d,e). We therefore expect the fibrous superstructure to significantly contribute to the measured anisotropy of the field-effect mobility. In addition, anisotropic transport within ordered LC domains and columns might play a considerable role. When zooming in on an *individual fibril* (Figure 4f), unidirectionally ordered *columnar* stacks are observed. The structural analysis, using WAXS and AFM, therefore leads to the structure schematically depicted in Figure 4g. The *fibrils*, oriented perpendicularly to the magnetic field, consist of *molecular columns* that make an angle of roughly ±40° with the field direction and in which the individual HBC−Ph_{12} molecules are aligned along the magnetic field in an edge-on arrangement. Interestingly, very recently the structure of zone-cast HBC−$C_{12}H_{25}$ films was determined in which the discs have a herringbone-packing motif with opposite rotations of 39° between neighboring stacked columns: Breiby, D. W.; Bunk, O.; Pisula, W.; Sølling, T. I.; Tracz, A.; Pakula, T.; Müllen, K.; Nielsen, M. N. *J. Am. Chem. Soc.* **2005**, *127*, 11288−11293. The anisotropic internal structure of the fibrils might be an extra contribution to the ultrahigh anisotropy of μ_{FE}.

Conclusions

We have demonstrated in the case of substituted hexabenzocoronenes that magnetic fields are effective for producing oriented films of discotic liquid-crystalline materials. This allows the investigation of structure−property relationships in such magnetically aligned films formed in transistor structures in a noninvasive, contact-free way. We find that the field-effect mobility in magnetically aligned films is more than 10 times higher than that in isotropic films, which highlights the importance of controlling the active material's microstructure for achieving optimum device performance. Since magnetic field alignment is applicable to a wide variety of self-assembled systems, this method is a promising tool for optimizing the properties of functional materials. Currently, we are optimizing the fabrication conditions in order to lower the magnetic fields and utilizing materials that have a higher intrinsic charge-carrier mobility to enhance the device performance.[30]

Experimental Methods

Magnetic Field Alignment. Alignment experiments were performed in a water-cooled, 20 T, resistive Bitter magnet, the operation of which is discussed elsewhere.[31] The temperature of the sample was stabilized at 20 °C (±0.1 °C) using a water-based temperature controller.

WAXS. Wide-angle X-ray scattering was carried out using a custom-built setup for experiments in reflection mode. Monochromatic Cu Kα radiation was employed. Pole figures were recorded at a fixed scattering angle (constant d-spacing) measuring a series of φ-scans (in-plane rotation around the center of the sample) at various tilt angles, ψ (azimuth angles).

AFM. Atomic force microscopy images were recorded under ambient conditions using a Digital Instrument Multimode Nanoscope IV, operating in the tapping mode regime on the FET devices immediately after mobility measurements. Microfabricated silicon cantilever tips (NSG01), with a resonance frequency of approximately 150 kHz and a spring constant of about 5.5 Nm^{-1}, were used. The scan rate varied from 0.5 to 1.5 Hz. The set-point amplitude ratio ($r_{sp} = A_{sp}/A_o$, where A_{sp} is the amplitude set point and A_o is the amplitude of the free oscillation) was adjusted to 0.75. All AFM images shown here were subjected to a first-order plane-fitting procedure to compensate for sample tilt. AFM analysis was done offline.

Devices. The field-effect transistor devices consisted of heavily doped Si wafers as the gate electrode, covered by a 200 nm thick layer of thermally oxidized SiO_2. Using conventional lithography, 100 nm thick

(29) Meijer, E. J.; Gelinck, G. H.; van Veenendaal, E.; Huisman, B.-H.; de Leeuw, D. M.; Klapwijk, T. M. *Appl. Phys. Lett.* **2003**, *82*, 4576−4578.
(30) Piris, J.; Debije, M. G.; Watson, M. D.; Müllen, K.; Warman, J. M. *Adv. Funct. Mater.* **2004**, *14*, 1047−1052.
(31) Perenboom, J. A. A. J.; Wiegers S. A. J.; Christianen P. C. M.; Zeitler, U.; Maan, J. C. *Physica B* **2004**, *346*, 659−662.

gold source and drain contacts were defined, with channel widths ranging from 1 mm to 1 cm and channel lengths between 0.75 and 40 μm. Two sets of contact series were prepared at orthogonal directions to each other. This allowed the determination of the charge transport characteristics parallel (denoted by ||) and perpendicular ($\perp$) to the magnetic field on one single wafer. All device characteristics were measured at 40 °C, in the dark, and at a pressure of 10^{-3} mbar, using a HP4155B semiconductor parameter analyzer.

Acknowledgment. This work is part of the research programs of the "Stichting voor Fundamenteel Onderzoek der Materie (FOM)", and the Council for the Chemical Sciences (CW), financially supported by the Netherlands Organisation for Scientific Research (NWO). N.S. is very grateful to the Swiss Federal Office for Education and Science for a post-doctoral fellowship in the frame of the EU-research-program IHP (HPMI-CT-2001-00146; BBW Nr. 02.0428). The MPIP group thanks the financial support from EU Project NAIMO (NMP4-CT-2004-500355).

JA054694T